

Neuroimaging

Probability of Alzheimer's disease in breast cancer survivors based on gray-matter structural network efficiency

Shelli R. Kesler^{a,*}, Vikram Rao^a, William J. Ray^b, Arvind Rao^c, and the Alzheimer's Disease Neuroimaging Initiative¹

^aDepartment of Neuro-oncology, University of Texas MD Anderson Cancer Center, Houston, TX, USA

^bThe Neurodegeneration Consortium at the Institute of Applied Cancer Science, University of Texas MD Anderson Cancer Center, Houston, TX, USA

^cDepartment of Bioinformatics and Computational Biology, University of Texas MD Anderson Cancer Center, Houston, TX, USA

Abstract

Introduction: Breast cancer chemotherapy is associated with accelerated aging and potentially increased risk for Alzheimer's disease (AD).

Methods: We calculated the probability of AD diagnosis from brain network and demographic and genetic data obtained from 47 female AD converters and 47 matched healthy controls. We then applied this algorithm to data from 78 breast cancer survivors.

Results: The classifier discriminated between AD and healthy controls with 86% accuracy ($P < .0001$). Chemotherapy-treated breast cancer survivors demonstrated significantly higher probability of AD compared to healthy controls ($P < .0001$) and chemotherapy-naïve survivors ($P = .007$), even after stratifying for apolipoprotein e4 genotype. Chemotherapy-naïve survivors also showed higher AD probability compared to healthy controls ($P = .014$).

Discussion: Chemotherapy-treated breast cancer survivors who have a particular profile of brain structure may have a higher risk for AD, especially those who are older and have lower cognitive reserve.

© 2017 The Authors. Published by Elsevier Inc. on behalf of the Alzheimer's Association. This is an open access article under the CC BY-NC-ND license (<http://creativecommons.org/licenses/by-nc-nd/4.0/>).

Keywords:

Breast cancer; Chemotherapy; Connectome; Alzheimer's disease; MRI

1. Introduction

Alzheimer's disease (AD) is the most common form of age-related neurodegeneration [1]. Age is the most consistent predictor of AD [2] and is also a primary risk factor

for cancer. Approximately one in two adults will be diagnosed with cancer during their lifetime with a median age at diagnosis of 66 years. Advances in cancer treatments, such as chemotherapy, have resulted in significantly improved survival rates leading to a large and growing cohort of chemotherapy-exposed older adults. Although most cancer diagnoses originate outside the central nervous system (CNS), cancer and its treatments have been associated with significant cognitive decline. Although estimates vary widely due to differences in methodology, cognitive impairment is a significant side effect of cancer and its treatments that can persist for decades or more beyond treatment cessation [3].

As suggested previously by other groups [4,5], many of the candidate mechanisms for chemotherapy-related cognitive impairment overlap those associated with aging and

The authors have declared that no conflict of interest exists.

¹Data used in preparation of this article were obtained from the Alzheimer's Disease Neuroimaging Initiative (ADNI) database (adni.loni.usc.edu). As such, the investigators within the ADNI contributed to the design and implementation of ADNI and/or provided data but did not participate in analysis or writing of this report. A complete listing of ADNI investigators can be found at: http://adni.loni.usc.edu/wp-content/uploads/how_to_apply/ADNI_Acknowledgement_List.pdf.

*Corresponding author. Tel.: +713-792-8296; Fax: +713-794-4999.

E-mail address: skesler@mdanderson.org

<https://doi.org/10.1016/j.dadm.2017.10.002>

2352-8729/© 2017 The Authors. Published by Elsevier Inc. on behalf of the Alzheimer's Association. This is an open access article under the CC BY-NC-ND license (<http://creativecommons.org/licenses/by-nc-nd/4.0/>).

neurodegeneration, therefore chemotherapy may alter or accelerate the brain aging trajectory. However, few have actually evaluated these concepts empirically. Ahles et al. [6] showed that older patients tend to have poorer cognitive outcome after chemotherapy. Koppelmans et al. [7] demonstrated that gray-matter atrophy after chemotherapy is analogous to approximately 4 years of aging on the brain. Sanoff et al. [8] showed that elevated expression of age-related molecular markers after chemotherapy corresponds to approximately 15 years of chronological aging. We previously demonstrated that chemotherapy-treated patients have significantly decreased resilience to computationally simulated brain aging compared to age-matched peers [9].

These results indicate that an AD-like profile of brain injury could be present early in some breast cancer survivors, increasing their risk for ongoing neurodegeneration and possible AD diagnosis [4]. However, no studies to date have directly compared AD and cancer chemotherapy in terms of their effects on brain structure or function. Some epidemiologic studies provide support for an increased risk of AD after breast cancer chemotherapy while others do not with methodological issues making definitive conclusions difficult [10]. Neuroimaging biomarkers may improve our ability to determine if cancer survivors are at higher risk for AD. Measures of brain network connectivity are especially promising for AD detection and risk assessment. For example, alterations in brain network connectivity have been shown to precede hallmark molecular changes associated with AD [11] and are highly accurate predictors of AD diagnosis and progression [12].

In this study, we applied graph theoretical analysis to measure structural brain networks. Graph theory is the study of objects and their connections and, when applied to neuroimaging data, provides unique metrics of brain network organization. In this context, the brain network is also known as the “connectome” and demonstrates a “small-world” topology where most regions are connected to their neighbors and can be reached by every other region via a small number of steps [13]. Efficient information processing is assumed to follow the shortest paths between regions; this efficiency can be measured at the global and local levels [14].

Connectomes can be constructed using coordinated variations in gray-matter volumes. These structural covariance networks are believed to reflect underlying axonal connections as well as common genetic, neurotropic, and neuroplastic processes [15]. Significant alterations in structural covariance networks have been observed in individuals with AD [16]. We have demonstrated that cognitive impairment is also associated with disruption of gray-matter structural networks in breast cancer survivors [17].

Machine-learning analysis of anatomic neuroimaging data can be used to discriminate between individuals with rapidly versus slowly progressive AD, predict future cognitive decline, and predict which patients with mild cognitive impairment (MCI) will convert to AD [18,19]. These methods are critical considering that the pathology of AD

is believed to begin many years before diagnosis [1]. Using regional connectome efficiencies in addition to demographic and genetic data, we aimed to identify a machine-learning algorithm that would accurately discriminate between healthy female controls and females with MCI who later converted to AD (i.e., had early disease). We then applied this algorithm to data obtained from a sample of breast cancer survivors, some with and some without a history of chemotherapy treatment. This approach allowed us to compute a probability of AD for each participant, which we then compared between groups. Our hypothesis was that chemotherapy-treated patients would have a higher probability of AD compared to chemotherapy-naïve patients.

2. Methods

2.1. Participants

Data for patients with primary breast cancer who received no CNS-directed therapies ($N = 108$) were retrospectively obtained from a prior study conducted by our laboratory focused on cognitive dysfunction and neuroimaging biomarkers in long-term breast cancer survivors.

We included only those participants who had magnetic resonance imaging (MRI) data and available apolipoprotein (*APOE*) genotype ($N = 78$). Of these, 40 had a history of chemotherapy treatment and 38 were chemotherapy naïve. Breast cancer survivors were enrolled only if they had completed adjuvant therapy at least 6 months prior to allow for neurologic and medical stabilization. The sample excluded participants with histories of neurologic, medical, or psychiatric conditions known to affect cognition. Breast cancer groups (chemotherapy, chemotherapy naïve) were frequency-matched for relevant treatment variables (Table 1).

Data for female AD converters were obtained from the Alzheimer's Disease Neuroimaging Initiative (ADNI) database (<http://adni.loni.usc.edu>). The ADNI was launched in 2003 as a public-private partnership, led by a principal investigator Michael W. Weiner, MD. The primary goal of ADNI has been to test whether serial MRI, positron emission tomography, other biological markers, and clinical and neuropsychological assessment can be combined to measure the progression of MCI and early AD. We obtained all available baseline ADNI data for females with MCI who later converted to AD who had volumetric MRI acquired using a 3-Tesla MRI scanner and had *APOE* genotype information. Exclusion criteria are described in [Supplementary Materials](#) and resulted in 47 AD converters. ADNI clinical characterization methods are described elsewhere [20].

Healthy female controls were women with no history of significant medical or psychological syndromes based on self-report and screening instruments [18–20]. We randomly selected healthy female control data taken from each data source to create a healthy control sample of $N = 47$ with 24 from ADNI and 23 from our data set (see [Supplementary Materials](#)). We combined healthy female

Table 1
Demographic and medical data shown as mean (standard deviation) unless otherwise indicated

Data	Chemotherapy	Chemotherapy naïve	Healthy females	AD converters
Age	54.9 (7.0)	58.4 (7.4)	68.2 (7.1)* [†]	68.6 (6.9)* [†]
Age range	43–73	41–74	56–79	55–80
Education (years)	16.3 (3.0)	16.7 (2.3)	16.0 (2.6)	15.6 (2.4)
<i>APOE</i> ε4	33% [‡]	24% [‡]	30% [‡]	72%
Time to AD conversion (months)				21.2 (12.7), range: 6–48
Postmenopausal	89%	80%		
Radiation therapy	73%	65%		
Endocrine therapy	45%	54%		
Stage at diagnosis (0, I, II, III) [§]	0%, 25%, 55%, 20%	40%, 49%, 16%, 0%		
Time since treatment completion (months)	56 (60)	76 (71)		
CAD total score [¶]	52 (11)	45 (11)		
MHD [#]	1.48 (0.68)	1.46 (0.79)		

Abbreviations: AD, Alzheimer's disease; *APOE* ε4, apolipoprotein ε4 genotype.

*Significantly ($P < .05$) different from chemotherapy.

[†]Significantly ($P < .05$) different from chemotherapy naïve.

[‡]Significantly ($P < .05$) different from AD converters.

[§]Stage at diagnosis differed significantly between the breast cancer groups ($P < .0001$).

[¶]Higher Clinical Assessment of Depression (CAD) score = greater symptoms of psychological distress/fatigue.

[#]Higher Mahalanobis distance (MHD) score = greater cognitive dysfunction.

data from both data sets to help control for subtle differences in neuroimaging data due to variations in MRI pulse sequences between the data sets. Healthy females were frequency-matched in terms of demographic data with the AD converter group (Table 1). This study was approved by the institutional review board of the University of Texas MD Anderson Cancer Center and was conducted in accordance with the Declaration of Helsinki. All participants provided written informed consent.

2.2. MRI acquisition

High-resolution, 3D, fast-spoiled gradient echo or magnetization-prepared rapid gradient echo T1-weighted MRI data were acquired for all participants using a GE, Philips, or Siemens 3-Tesla scanner. Scan parameters for our data set included slice thickness = 1.5 mm, field of view = 24 cm, matrix = 256×256 [21,22]. For ADNI, slice thickness = 1.2 mm, field of view = 24 or 26 cm, matrix = 240×256 , or 256×256 [23].

2.3. Structural connectome construction

Gray-matter volumes were segmented from T1-weighted MRI using voxel-based morphometry (VBM) via VBM8 Toolbox in Statistical Parametric Mapping 8 (SPM8) [24]. Custom templates for each group were created using a fast diffeomorphic registration algorithm (i.e., DARTEL) [25]. Successful normalization was confirmed via visual inspection using the check registration function in SPM8 as well as with whole-volume slice montages. Normalized image quality was further evaluated with the check sample homogeneity function in VBM8 Toolbox.

Gray-matter covariance networks were constructed for each participant using a similarity-based extraction method

[26,27] (Extract Individual GM Networks Toolbox v20150902 https://github.com/bettytijms/Single_Subject_Grey_Matter_Networks). Network nodes were defined as $3 \times 3 \times 3$ voxel cubes spanning the entire gray-matter volume (i.e., 27 gray-matter values per cube). A correlation matrix was calculated across all pairs of nodes and binarized based on a threshold estimated from a random network and false discovery rate [26,28]. We ensured that no binarized matrices were disconnected (i.e., had isolated nodes). Matrices were then submitted to graph theoretical analysis using Brain Connectivity Toolbox [29] and our bNets Toolbox (<https://github.com/srkesler/bNets.git>) implemented in MATLAB v2014b (Mathworks, Inc, Natick, MA). Connectome metrics were calculated as described previously [26,27]. Specifically, efficiency is defined as the inverse of the average shortest path between nodes and is high when nodes can interact directly. Degree refers to the number of connections a node has indicating how much that node is interacting with other nodes in the network. Size reflects the number of nodes in the network. Nodes were assigned 1 of 90 Automated Anatomical Labeling Atlas (AAL) labels based on the node's voxel coordinates. Efficiency was calculated for each node as the average efficiency across all nodes with the same AAL label [26,27]. We have previously demonstrated impaired connectome efficiency associated with cancer and its treatments [9,27], and others have shown impaired efficiency in individuals with early AD [30].

2.4. *APOE* genotyping

The ε4 variant of the *APOE* gene is associated with increased risk for AD as well as increased risk for cognitive deficit associated with chemotherapy [31,32].

Saliva samples were obtained from participants with breast cancer and healthy controls in our data set using the

Oragene DNA OG-250 collection kit (DNA Genotek, Kanata, Ontario), and *APOE* was genotyped by polymerase chain reaction fragment length polymorphism analysis using Cfo I [33]. Genotyping for ADNI participants was done from blood samples using polymerase chain reaction followed by HhaI restriction [34]. DNA obtained from saliva is highly comparable to that obtained from blood [35] and less invasive for the participant.

2.5. Machine-learning classification of AD converters and healthy controls

We used random forest classification [36] using a standard approach: The square root of the number of features was split at each node, and an ensemble of 500 trees was grown by bootstrapping the features with replacement. The following features were included: 90 nodal efficiencies, age (years), education level (years), and *APOE* genotype (1 = presence of $\epsilon 4$ allele, 0 = no $\epsilon 4$ allele). Total brain volume, network degree, and network size were also included to control for effects of head size and graph defining properties [26]. Brain structure feature values are presented in Table 2.

Feature selection/reduction was conducted using a nested folds approach with the training set (A+B) consisting of a 60% random sample of the combined AD converter and healthy control data. Recursive feature elimination was conducted on this set with A = training data and B = testing data with leave-one-out cross-validation across 100 random partitions of A and B. Features that provided the best accuracy across these partitions were used to re-train a model on A+B with out-of-bag error estimation [37]. The resulting model was then applied to the held-out 40% sample to test classification accuracy. Accuracy significance was evaluated using a two-sided exact binomial test in addition to the area under the curve of the receiver operating characteristic. Feature importance was determined using mean decrease in Gini index [27].

2.6. AD probability for breast cancer survivors

We used the model fit from the random forest classification of AD converters and healthy controls to predict the

probability of AD class for each participant in the breast cancer group. We then conducted a pairwise Wilcoxon signed-rank test with false discovery rate correction, after correcting for age using linear regression, to determine the difference in AD probability between the groups.

2.7. Host and cancer treatment factors associated with AD probability in breast cancer survivors

Multivariate linear regression was used to explore the specific effects of age, psychological distress, fatigue, *APOE* genotype, education level, history of radiation therapy (1 = yes, 0 = no), history of hormonal blockade therapy (1 = yes, 0 = no), disease stage at diagnosis (0, 1, 2, 3), time since treatment completion (months), menopausal status (1 = postmenopausal, 0 = premenopausal), chemotherapy class (1 = anthracycline [68%], 0 = nonanthracycline) [38] and cognitive dysfunction on AD probability for breast cancer survivors. Psychological distress and fatigue were measured using the total score from the Clinical Assessment of Depression [9]. Cognitive dysfunction was measured using the Mahalanobis distance score [39] derived from a battery of standardized neuropsychological tests (see [Supplementary Materials](#)). Demographic and cognitive data were measured/acquired on the same day as the MRI scan. Treatment/medical data were obtained on the same day as the MRI when possible and were confirmed or calculated based on the MRI date as necessary via medical records review.

All machine-learning and other statistical analyses were performed in the R Statistical Package (R Foundation) including the “randomForest”, “caret”, and “area under the curve” libraries.

3. Results

3.1. Machine-learning classification of AD converters and healthy controls

The final random forest model retained 12 of 96 features including, in order of descending importance, total brain volume, *APOE*, right middle frontal gyrus efficiency, bilateral

Table 2
Values for brain structure features retained by random forest classification

Brain structure feature	Alzheimer's disease converters	Chemotherapy	Healthy females	Chemotherapy naïve
Total brain volume (mL)	1010 (87)	1169 (98)	1100 (122)	1174 (93)
Network degree	3341 (103)	3529 (98)	3455 (97)	3541 (82)
Network size	6931 (36)	6950 (27)	6940 (31)	6946 (22)
Brain network efficiencies				
Right middle frontal gyrus	0.852 (0.005)	0.860 (0.005)	0.857 (0.005)	0.860 (0.005)
Left gyrus rectus	0.845 (0.008)	0.854 (0.007)	0.852 (0.007)	0.857 (0.007)
Right gyrus rectus	0.853 (0.008)	0.863 (0.006)	0.861 (0.007)	0.866 (0.006)
Left middle temporal pole	0.852 (0.006)	0.860 (0.006)	0.857 (0.005)	0.861 (0.005)
Right hippocampus	0.851 (0.006)	0.858 (0.005)	0.857 (0.005)	0.859 (0.004)
Right putamen	0.845 (0.007)	0.853 (0.005)	0.850 (0.005)	0.852 (0.006)
Left anterior cingulate	0.850 (0.005)	0.859 (0.006)	0.855 (0.005)	0.859 (0.005)

gyrus rectus efficiency, network degree, left middle temporal pole efficiency, right hippocampus efficiency, right putamen efficiency, network size, left anterior cingulate efficiency, and age (Fig. 1).

The classifier demonstrated an accuracy of 86% ($P < .0001$) with sensitivity of 91% and specificity of 81% for a receiver operating characteristic of 0.96.

3.2. AD probability for breast cancer survivors

After the AD converter group, chemotherapy-treated breast cancer survivors had the highest AD probability, which was significantly higher than that of both chemotherapy-naïve survivors ($P = .007$) and healthy controls ($P < .0001$). The chemotherapy-naïve group also differed from healthy controls ($P = .014$, Fig. 2). The difference between chemotherapy and chemotherapy-naïve groups remained even after stratifying for *APOE* $\epsilon 4$ genotype ($W = 92$, $P = .025$, Fig. 2).

3.3. Host and cancer treatment factors associated with AD probability in breast cancer survivors

The linear regression model for chemotherapy-treated survivors demonstrated a significant adjusted $R^2 = 0.32$, $P = .029$. Education ($P = .044$) and *APOE* $\epsilon 4$ ($P = .006$) were the only significant factors (Supplementary Table 1). The model for chemotherapy-naïve survivors was not signif-

icant (adjusted $R^2 = 0.17$, $P = .74$) with no significant variables ($P > .110$, Supplementary Table 2).

4. Discussion

In this study, we aimed to evaluate the risk of AD in women with a history of breast cancer based on brain structure in combination with demographics and *APOE* genotype. We first determined a machine-learning algorithm that accurately discriminated between healthy women and women with MCI who later developed AD (AD converters). The classifier performed with 86% accuracy, consistent with similar previous studies of AD conversion [18,19]. We then applied the machine-learning algorithm to a separate sample of breast cancer survivors to predict individual probability of developing AD. Survivors with a history of chemotherapy treatment showed significantly higher AD probability compared to chemotherapy-naïve survivors as well as healthy female controls. Survivors without a history of chemotherapy also demonstrated higher AD probability compared to healthy controls. Thus, patients with breast cancer, especially those who received chemotherapy, may have an increased risk for AD.

Our results do not suggest that cancer or its treatments cause AD but point to shared risk factors including a common neural phenotype of brain structure alterations. We have previously demonstrated that breast cancer

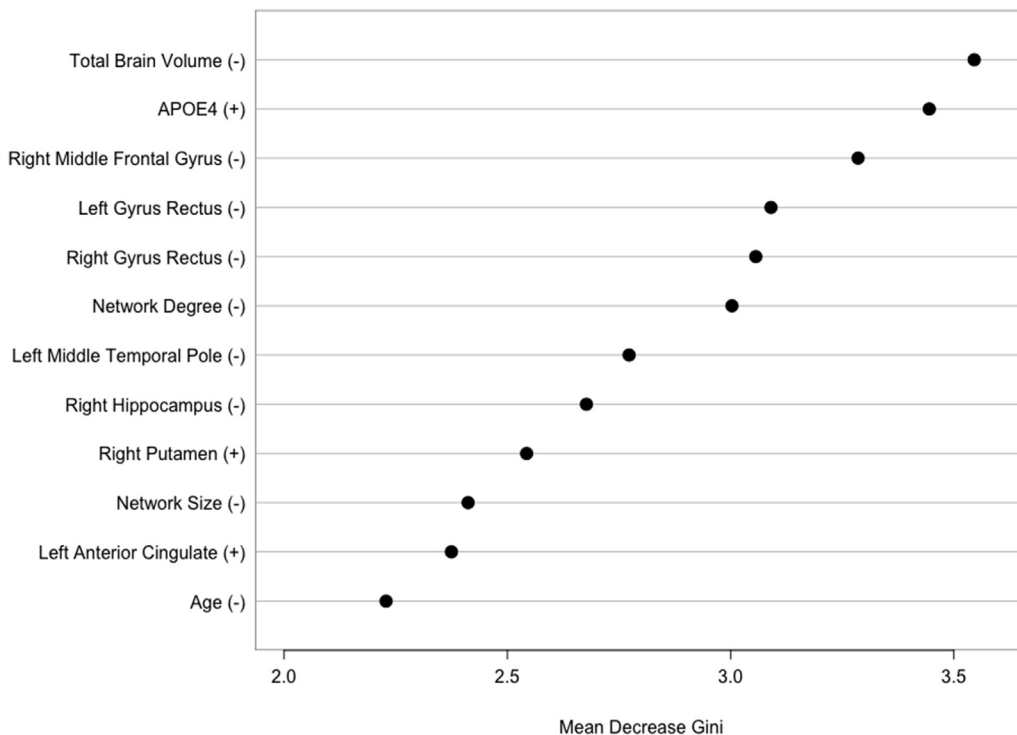


Fig. 1. Random forest classification of Alzheimer's disease (AD) converters and healthy female controls. Mean decrease in Gini index of features retained by the final model. Higher mean decrease in Gini index indicates greater importance of that feature in the model. +/- indicates the direction of the relationship of the feature with AD class, for example, lower total brain volume was associated with AD class. Abbreviation: APOE4 = apolipoprotein $\epsilon 4$ genotype.

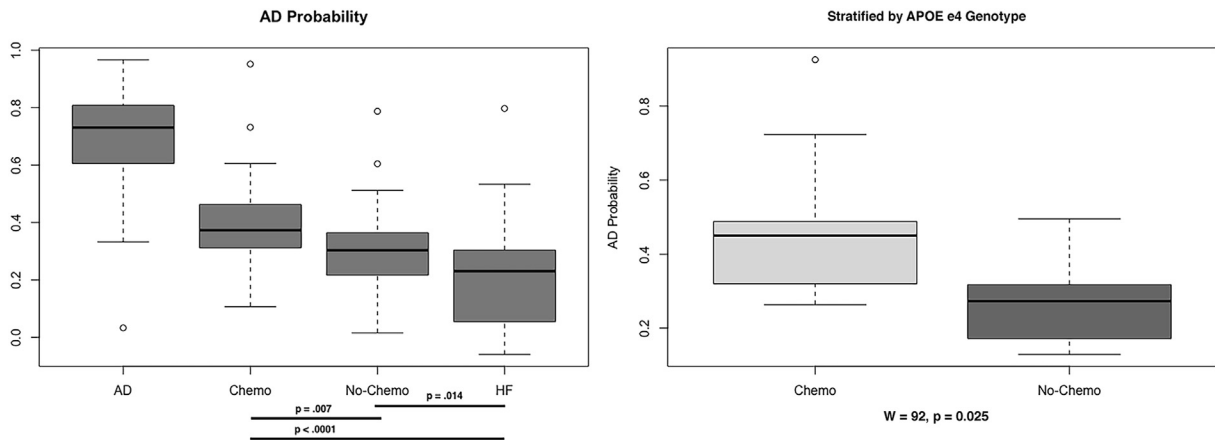


Fig. 2. Alzheimer's disease (AD) probability. The chemotherapy group demonstrated significantly higher AD probability compared to chemotherapy-naïve and healthy female (HF) groups even after stratifying for apolipoprotein (*APOE*) $\epsilon 4$ genotype.

chemotherapy and AD are qualitatively associated with a similar pattern of altered gray-matter structural network organization compared to age-matched peers [17]. Breast cancer and chemotherapy tend to injure brain regions that are known to be affected by AD including hippocampus, default mode network, prefrontal cortex, and white-matter pathways [9,22,40]. These regions were among those that we observed to discriminate between the AD and healthy control groups. Apart from right putamen and left anterior cingulate, lower regional efficiencies were associated with AD classification (Fig. 1). Total brain volume was the most important variable in the random forest classifier and has been shown to be atrophic in breast cancer survivors even decades after treatment completion [7]. These results suggest that women with a history of breast cancer treatment who demonstrate a particular profile of brain volume and regional efficiencies may be at increased risk for AD.

Our findings also indicate that chemotherapy-treated survivors who are older and have lower cognitive reserve are at increased risk, consistent with previous studies [6]. Interestingly, although age is the most consistent predictor of AD, our classifier results indicated that brain volume and regional brain network efficiencies were more critical for discriminating individuals with and without early AD. In addition, education demonstrated a positive relationship with AD probability in the chemotherapy group. This seemingly counterintuitive direction is well known in the cognitive reserve literature and is interpreted to reflect the higher threshold of brain injury required for clinical effects to be manifested in individuals with higher education levels [9]. Our breast cancer sample was relatively young and also highly educated, and therefore, these findings require replication in women who are older and have less cognitive reserve.

Breast cancer and/or chemotherapy may exacerbate an existing genetic risk for AD. Both cancer groups had higher AD probability than healthy controls. However, patients who had an *APOE* $\epsilon 4$ genotype and were treated with chemo-

therapy were at increased risk for AD compared to patients who had the *APOE* $\epsilon 4$ genotype but were not treated with chemotherapy. *APOE* $\epsilon 4$ genotypes are associated with increased amyloid β ($A\beta$) protein accumulation and tau hyperphosphorylation, the molecular triggers of the two primary forms of neuropathology in AD [41]. Both $A\beta$ precursor protein and tau are expressed by breast cancer cells [42,43], and preclinical studies suggest that administration of peripheral tau or $A\beta$ seeds results in tau or amyloid-related CNS pathologies, respectively [44,45]. We previously demonstrated that breast cancer chemotherapy impairs autophagy [46], which may exacerbate normal age-related weakening of clearance mechanisms, worsening accumulation of toxins such as $A\beta$ and tau. However, the effect of tau and $A\beta$ expression from breast cancer cells on the CNS is currently unknown. Novel methods for sensitively measuring tau and $A\beta$ from blood have been recently developed [47] making investigation of this question a possibility.

Increased risk for breast cancer diagnosis has been associated with the *APOE* $\epsilon 4$ genotype [48]. We conducted a post hoc, two-tailed Spearman correlation analysis that demonstrated a small effect association between *APOE* $\epsilon 4$ genotype and higher disease stage ($r = 0.21$, $P = .067$). This is consistent with previous work showing that $A\beta$ is more strongly expressed by breast cancer cell lines that have increased metastatic potential [42]. Our findings support those of previous studies suggesting that *APOE* genotype may be a valuable predictor of risk for breast cancer [48] as well as breast cancer-related cognitive impairment [31,32].

The main limitation of this study is the small sample size, which can result in model overfitting. We conducted random forest modeling using a conservative approach that included cross-validation and careful separation of training and testing samples. However, further evaluation of our models' validity requires a new, unseen, and larger sample of patients to which we can apply our algorithms. The retrospective,

cross-sectional design prevents us from evaluating the change in AD probability across the treatment course and therefore limits conclusions regarding the contribution of chemotherapy alone to our results. Although endocrine and radiation treatment histories were not associated with AD probability, we cannot completely rule out their roles based on this study. There are also potential confounds due to combination of neuroimaging data from various sites. We attempted to reduce these confounds by selecting only 3-Tesla data and by using a balanced sample of healthy controls from both retrospective data sets. In addition, ADNI has implemented rigorous methods to standardize their protocols across sites and scanner platforms [23].

However, this study provides a foundation for using machine-learning algorithms in combination with neuroimaging data to evaluate risk of progressive chemotherapy-related brain injury. We have made our random forest model available publicly so that others may test its application to their own data as appropriate (<https://www.dropbox.com/s/rjzpk5magq8gj3a/ADvCNfit.RData?dl=0>). Although we demonstrated that breast cancer survivors may have an increased risk for AD, it is unknown whether a history of breast cancer treatment accelerates AD onset and/or worsens its progression. These are important questions for larger studies of patients with breast cancer and/or preclinical studies using AD mouse models. While the parallel between AD and chemotherapy-related cognitive impairment is not original [4,5], our approach to examining this overlap is highly unique in the field. Future studies will combine AD probability with biomarkers of neurodegeneration such as tau, A β , and cytokine levels to better understand the mechanisms and consequences of chemotherapy-related cognitive impairment.

Acknowledgments

This research was funded by the National Cancer Institute (1R03CA191559, 1R01CA172145, and 1R01NR014195 to S.R.K.). Data collection and sharing for this project was funded by the Alzheimer's Disease Neuroimaging Initiative (ADNI) (National Institutes of Health grant U01 AG024904) and DOD ADNI (Department of Defense award number W81XWH-12-2-0012). ADNI is funded by the National Institute on Aging, the National Institute of Biomedical Imaging and Bioengineering, and through generous contributions from the following: AbbVie; Alzheimer's Association; Alzheimer's Drug Discovery Foundation; Araclon Biotech; BioClinica, Inc.; Biogen; Bristol-Myers Squibb Company; CereSpir, Inc.; Cogstate; Eisai Inc.; Elan Pharmaceuticals, Inc.; Eli Lilly and Company; EuroImmun; F. Hoffmann-La Roche Ltd. and its affiliated company Genentech, Inc.; Fujirebio; GE Healthcare; IXICO Ltd.; Janssen Alzheimer Immunotherapy Research & Development, LLC.; Johnson & Johnson Pharmaceutical Research & Development LLC.; Lumosity; Lundbeck; Merck & Co., Inc.; Meso Scale Diagnostics, LLC.; NeuroRx Research; Neurotrack Technologies; Novartis Pharmaceuticals Corporation; Pfizer Inc.; Piramal Imaging;

Servier; Takeda Pharmaceutical Company; and Transition Therapeutics. The Canadian Institutes of Health Research is providing funds to support ADNI clinical sites in Canada. Private sector contributions are facilitated by the Foundation for the National Institutes of Health (www.fnih.org). The grantee organization is the Northern California Institute for Research and Education, and the study is coordinated by the Alzheimer's Therapeutic Research Institute at the University of Southern California. ADNI data are disseminated by the Laboratory for Neuro Imaging at the University of Southern California. The authors wish to thank Joachim Hallmayer, PhD, for assistance with genetic analysis. The funding source had no role in study design; in the collection, analysis, and interpretation of data; in the writing of the report; or in the decision to submit the article for publication.

Supplementary data

Supplementary data related to this article can be found at <https://doi.org/10.1016/j.dadm.2017.10.002>.

RESEARCH IN CONTEXT

1. Systematic review: The authors reviewed the literature using traditional scientific sources (e.g., PubMed) for research regarding cognition, neuroimaging, breast cancer, and Alzheimer's disease (AD). Although previous studies have demonstrated evidence of accelerated brain aging associated with breast cancer chemotherapy, the risk for AD has not been evaluated from a neurobiologic perspective.
2. Interpretation: Using machine learning, we showed that chemotherapy-treated patients have higher AD probability compared to chemotherapy-naïve patients based on brain structure, demographics, and genotype. We conclude that chemotherapy increases existing genetic risk for AD.
3. Future directions: Further investigation is required to determine if chemotherapy worsens AD onset and/or progression, to evaluate the effects of tumor pathology and chemotherapy on tau and A β accumulation, and to examine the potential contributions of other adjuvant therapies such as radiation and endocrine treatments.

References

- [1] Risacher SL, Saykin AJ. Neuroimaging and other biomarkers for Alzheimer's disease: the changing landscape of early detection. *Annu Rev Clin Psychol* 2013;9:621-48.

- [2] Kravitz E, Schmeidler J, Beeri MS. Cognitive decline and dementia in the oldest-old. *Rambam Maimonides Med J* 2012;3:e0026.
- [3] Wefel JS, Kesler SR, Noll KR, Schagen SB. Clinical characteristics, pathophysiology, and management of noncentral nervous system cancer-related cognitive impairment in adults. *CA Cancer J Clin* 2015;65:123–38.
- [4] Mandelblatt JS, Hurria A, McDonald BC, Saykin AJ, Stern RA, VanMeter JW, et al. Cognitive effects of cancer and its treatments at the intersection of aging: what do we know; what do we need to know? *Semin Oncol* 2013;40:709–25.
- [5] Ahles TA. Brain vulnerability to chemotherapy toxicities. *Psychoncology* 2012;21:1141–8.
- [6] Ahles TA, Saykin AJ, McDonald BC, Li Y, Furstenberg CT, Hanscom BS, et al. Longitudinal assessment of cognitive changes associated with adjuvant treatment for breast cancer: impact of age and cognitive reserve. *J Clin Oncol* 2010;28:4434–40.
- [7] Koppelmans V, de Ruiter MB, van der Lijn F, Boogerd W, Seynaeve C, van der Lugt A, et al. Global and focal brain volume in long-term breast cancer survivors exposed to adjuvant chemotherapy. *Breast Cancer Res Treat* 2012;132:1099–106.
- [8] Sanoff HK, Deal AM, Krishnamurthy J, Torrice C, Dillon P, Sorrentino J, et al. Effect of cytotoxic chemotherapy on markers of molecular age in patients with breast cancer. *J Natl Cancer Inst* 2014;106:dju057.
- [9] Kesler SR, Watson CL, Blayney DW. Brain network alterations and vulnerability to simulated neurodegeneration in breast cancer. *Neurobiol Aging* 2015;36:2429–42.
- [10] Koppelmans V, Breteler MM, Boogerd W, Seynaeve C, Schagen SB. Late effects of adjuvant chemotherapy for adult onset non-CNS cancer; cognitive impairment, brain structure and risk of dementia. *Crit Rev Oncol Hematol* 2013;88:87–101.
- [11] Sheline YI, Morris JC, Snyder AZ, Price JL, Yan Z, D'Angelo G, et al. APOE4 allele disrupts resting state fMRI connectivity in the absence of amyloid plaques or decreased CSF Aβ42. *J Neurosci* 2010;30:17035–40.
- [12] Tuladhar AM, van Uden IW, Rutten-Jacobs LC, Lawrence A, van der Holst H, van Norden A, et al. Structural network efficiency predicts conversion to dementia. *Neurology* 2016;86:1112–9.
- [13] Bassett DS, Bullmore E. Small-world brain networks. *Neuroscientist* 2006;12:512–23.
- [14] Achard S, Bullmore E. Efficiency and cost of economical brain functional networks. *PLoS Comput Biol* 2007;3:e17.
- [15] Alexander-Bloch A, Giedd JN, Bullmore E. Imaging structural covariance between human brain regions. *Nat Rev Neurosci* 2013;14:322–36.
- [16] Tijms BM, Kate MT, Wink AM, Visser PJ, Ecay M, Clerigue M, et al. Gray matter network disruptions and amyloid beta in cognitively normal adults. *Neurobiol Aging* 2016;37:154–60.
- [17] Hosseini SM, Koovakkattu D, Kesler SR. Altered small-world properties of gray matter networks in breast cancer. *BMC Neurol* 2012;12:28.
- [18] Moradi E, Pepe A, Gaser C, Huttunen H, Tohka J, Alzheimer's Disease Neuroimaging I. Machine learning framework for early MRI-based Alzheimer's conversion prediction in MCI subjects. *NeuroImage* 2015;104:398–412.
- [19] Gaser C, Franke K, Kloppel S, Koutsouleris N, Sauer H, Alzheimer's Disease Neuroimaging I. BrainAGE in mild cognitive impaired patients: predicting the conversion to Alzheimer's disease. *PLoS One* 2013;8:e67346.
- [20] Petersen RC, Aisen PS, Beckett LA, Donohue MC, Gamst AC, Harvey DJ, et al. Alzheimer's Disease Neuroimaging Initiative (ADNI): clinical characterization. *Neurology* 2010;74:201–9.
- [21] Kesler SR, Wefel JS, Hosseini SM, Cheung M, Watson CL, Hoefl F. Default mode network connectivity distinguishes chemotherapy-treated breast cancer survivors from controls. *Proc Natl Acad Sci U S A* 2013;110:11600–5.
- [22] Kesler S, Janelsins M, Koovakkattu D, Palesh O, Mustian K, Morrow G, et al. Reduced hippocampal volume and verbal memory performance associated with interleukin-6 and tumor necrosis factor-alpha levels in chemotherapy-treated breast cancer survivors. *Brain Behav Immun* 2013;30:S109–16.
- [23] Jack CR, Bernstein MA, Fox NC, Thompson P, Alexander G, Harvey D, et al. The Alzheimer's disease neuroimaging initiative (ADNI): MRI methods. *J Magn Reson Imaging* 2008;27:685–91.
- [24] Kurth F, Gaser C, Luders E. A 12-step user guide for analyzing voxel-wise gray matter asymmetries in statistical parametric mapping (SPM). *Nat Protoc* 2015;10:293–304.
- [25] Ashburner J. A fast diffeomorphic image registration algorithm. *NeuroImage* 2007;38:95–113.
- [26] Tijms BM, Series P, Willshaw DJ, Lawrie SM. Similarity-based extraction of individual networks from gray matter MRI scans. *Cereb Cortex* 2012;22:1530–41.
- [27] Kesler SR, Noll K, Cahill DP, Rao G, Wefel JS. The effect of IDH1 mutation on the structural connectome in malignant astrocytoma. *J Neurooncol* 2017;131:565–74.
- [28] Noble WS. How does multiple testing correction work? *Nat Biotechnol* 2009;27:1135–7.
- [29] Rubinov M, Sporns O. Complex network measures of brain connectivity: uses and interpretations. *NeuroImage* 2010;52:1059–69.
- [30] Fischer FU, Wolf D, Scheurich A, Fellgiebel A, Alzheimer's Disease Neuroimaging I. Altered whole-brain white matter networks in pre-clinical Alzheimer's disease. *NeuroImage Clin* 2015;8:660–6.
- [31] Kolecck TA, Bender CM, Sereika SM, Ahrendt G, Jankowitz RC, McGuire KP, et al. Apolipoprotein E genotype and cognitive function in postmenopausal women with early-stage breast cancer. *Oncol Nurs Forum* 2014;41:E313–25.
- [32] Ahles TA, Li Y, McDonald BC, Schwartz GN, Kaufman PA, Tsongalis GJ, et al. Longitudinal assessment of cognitive changes associated with adjuvant treatment for breast cancer: the impact of APOE and smoking. *Psychooncology* 2014;23:1382–90.
- [33] Ota M, Fukushima H, Kulski JK, Inoko H. Single nucleotide polymorphism detection by polymerase chain reaction-restriction fragment length polymorphism. *Nat Protoc* 2007;2:2857–64.
- [34] Saykin AJ, Shen L, Foroud TM, Potkin SG, Swaminathan S, Kim S, et al. Alzheimer's Disease Neuroimaging Initiative biomarkers as quantitative phenotypes: Genetics core aims, progress, and plans. *Alzheimers Dement* 2010;6:265–73.
- [35] Bahlo M, Stankovich J, Danoy P, Hickey PF, Taylor BV, Browning SR, et al. Saliva-derived DNA performs well in large-scale, high-density single-nucleotide polymorphism microarray studies. *Cancer Epidemiol Biomarkers Prev* 2010;19:794–8.
- [36] Breiman L. Random forests. *Machine Learn* 2001;45:5–32.
- [37] Liaw A, Wiener M. Classification and Regression by randomForest. *R News* 2002;2:18–22.
- [38] Kesler SR, Blayney DW. Neurotoxic effects of anthracycline- vs nonanthracycline-based chemotherapy on cognition in breast cancer survivors. *JAMA Oncol* 2016;2:185–92.
- [39] Mahalanobis PC. On the generalised distance in statistics. *Proc Natl Inst Sci India* 1936;2:49–55.
- [40] Miao H, Chen X, Yan Y, He X, Hu S, Kong J, et al. Functional connectivity change of brain default mode network in breast cancer patients after chemotherapy. *Neuroradiology* 2016;58:921–8.
- [41] Lloret A, Fuchsberger T, Giraldo E, Vina J. Molecular mechanisms linking amyloid beta toxicity and Tau hyperphosphorylation in Alzheimer's disease. *Free Radic Biol Med* 2015;83:186–91.
- [42] Lim S, Yoo BK, Kim H-S, Gilmore HL, Lee Y, Lee HP, et al. Amyloid-β precursor protein promotes cell proliferation and motility of advanced breast cancer. *BMC Cancer* 2014;14:928.
- [43] Bonneau C, Gurard-Levin Z, Andre F, Pusztaï L, Rouzier R. Predictive and prognostic value of the TauProtein in breast cancer. *Anticancer Res* 2015;35:5179–84.
- [44] Clavaguera F, Hench J, Lavenir I, Schweighauser G, Frank S, Goedert M, et al. Peripheral administration of tau aggregates triggers intracerebral tauopathy in transgenic mice. *Acta Neuropathol* 2014;127:299.

- [45] Eisele YS, Obermuller U, Heilbronner G, Baumann F, Kaeser SA, Wolburg H, et al. Peripherally applied Abeta-containing inoculates induce cerebral beta-amyloidosis. *Science* 2010;330:980–2.
- [46] Manchon J, Uzor N, Kesler S, Wefel J, Townley A, Pradeep S, et al. TFEB ameliorates the impairment of the autophagy-lysosome pathway in neurons induced by doxorubicin. *Aging* 2016;8:3507–19.
- [47] Bogoslovsky T, Wilson D, Chen Y, Hanlon D, Gill J, Jeromin A, et al. Increases of plasma levels of glial fibrillary acidic protein, tau, and amyloid beta up to 90 days after traumatic brain injury. *J Neurotrauma* 2017;34:66–73.
- [48] Cibeira GH, Giacomazzi J, Aguiar E, Schneider S, Ettrich B, DE Souza CI, et al. Apolipoprotein E genetic polymorphism, serum lipoprotein levels and breast cancer risk: a case-control study. *Mol Clin Oncol* 2014;2:1009–15.